Proceedings of FEDSM06
ASME 2006 Fluids Engineering Conference&
7th International Symposium on Numerical Methods for Multiphase Flows
July 17-20, 2006, Miami, USA

FEDSM2006-98447

A LATTICE BOLTZMANN EQUATION METHOD WITHOUT PARASITIC CURRENTS AND ITS APPLICATION IN DROPLET COALESCENCE

Taehun Lee*
Mathematics and Computer Science Division
Argonne National Laboratory
Argonne, Illinois 60439
& Department of Mechanical Engineering
The City College of the City University of New York
New York, New York 10031
Email: thlee@ccny.cuny.edu

Paul F. Fischer
Mathematics and Computer Science Division
Argonne National Laboratory
Argonne, Illinois 60439
Email: fischer@mcs.anl.gov

ABSTRACT

A formulation of the intermolecular force in the nonideal gas lattice Boltzmann equation (LBE) method is examined. Discretization errors in the computation of the intermolecular force cause parasitic currents. The parasitic currents can be eliminated to round-off if the potential form of the intermolecular force is used with compact isotropic discretization. Numerical tests confirm the elimination of the parasitic currents. In order to demonstrate the applicability of the present model, inertial coalescence of droplets at high density ratio is studied.

INTRODUCTION

The lattice Boltzmann equation (LBE) methods for nonideal gases or binary fluids have witnessed significant progress in recent years [1–7]. The success of LBE methods can largely be attributed to their mesoscopic and kinetic nature, which enables the simulation of the macroscopic interfacial dynamics with the underlying microscopic physics. On the macroscopic level, most of these two-phase LBE methods can be considered as diffuse interface methods [8] in that the phase interface is spread on grid points and the surface tension is transformed into a volumetric force. Generally, diffuse interface methods have some advantages over sharp interface methods because computations are much easier for three-dimensional (3-D) flows in which topological change of the interfaces is complicated. When applied on the uniform grid, LBE methods enjoy the unit CFL (Courant, Friedrichs, and Lewy) property that eliminates any numerical errors involved in the computation of the advection operator. The inherent isotropy of the lattice guarantees isotropic discretization of the differential operators in LBE. Free from advection errors and anisotropic discretization, the LBE method can deliver much improved solutions with the same grid resolution.

One undesirable feature of LBE methods as a diffuse interface method is the existence of parasitic currents. The parasitic currents are small-amplitude velocity fields caused by a slight imbalance between stresses in the interfacial region [9]. These currents increase as the surface tension force and can be reduced with large viscous dissipation, but never disappear in most cases. In the case of a 2-D liquid droplet immersed in a vapor phase, the flow tends to be organized into eight eddies with centers lying on the interface. In the diffuse interface method, the key to reducing the parasitic currents lies in the formulation of the surface tension force. Jacqmin [10] suggested that the potential form of the surface tension force was guaranteed to generate motionless equilibrium states without parasitic currents. Jamet *et al.* [11] later showed that the potential form ensured the correct energy transfer between the kinetic energy and the surface tension energy, eliminating parasitic currents.

*Address all correspondence to this author.

Several attempts have been made to reduce the magnitude of the parasitic currents and identify their origins [12–14] in the LBE framework. Nourgaliev *et al*. [12] employed a finite difference approach in the streaming step of LBE and reported reduced currents compared with the previous LBE methods. Lishchuk *et al*. [13] noted that the parasitic currents were unwanted artifacts originating from the mesoscopic (or microscopic) nature of LBE having the interface with a finite thickness, and they tried to incorporate sharp interface kinematics into their LBE method. Cristea and Sofonea [14] argued that the directional derivative operator $\mathbf{e}_\alpha \cdot \nabla$ in LBE (see Eq. (1)) generated the parasitic currents in the interfacial region, and consequently, they concluded that the parasitic currents would be reduced by the surface tension force. All these LBE schemes were able to reduce the magnitude of the parasitic currents to a certain degree but never made them entirely disappear.

The discrete Boltzmann equation (DBE) proposed by He *et al*. [5] will be analyzed, but the analysis is equally valid for other LBE methods. We will show that the potential form of the intermolecular force in the LBE context eliminates the parasitic currents. In order to demonstrate the applicability of the present model, inertial coalescence of droplets will be examined.

NOMENCLATURE

f_α Particle distribution function
f_α^{eq} Equilibrium distribution function
$\mathbf{e}_\alpha$ Microscopic particle velocity
$\mathbf{u}$ Macroscopic velocity
ρ Density
c_s Speed of sound
λ Relaxation time
τ Nondimensional relaxation time
t_α Weighting factor
$\mathbf{F}$ Intermolecular force
κ Gradient parameter
p_0 Thermodynamic pressure
E_{mix} Mixing energy
E_0 Bulk energy
μ_0 Chemical potential
D Interface thickness
σ Surface tension
ν Kinematic viscosity
R_0 Radius of a droplet

THEORY

The DBE with external force $\mathbf{F}$ can be written as

$$\frac{\partial f_\alpha}{\partial t} + \mathbf{e}_\alpha \cdot \nabla f_\alpha = -\frac{f_\alpha - f_\alpha^{eq}}{\lambda} + \frac{(\mathbf{e}_\alpha - \mathbf{u}) \cdot \mathbf{F}}{\rho c_s^2} f_\alpha^{eq}, \qquad (1)$$

where f_α is the particle distribution function, $\mathbf{e}_\alpha$ is the microscopic particle velocity, $\mathbf{u}$ is the macroscopic velocity, ρ is the density, c_s is a constant, and λ is the relaxation time. The equilibrium distribution function f_α^{eq} is given by

$$f_\alpha^{eq} = t_\alpha \rho \left[1 + \frac{\mathbf{e}_\alpha \cdot \mathbf{u}}{c_s^2} + \frac{(\mathbf{e}_\alpha \cdot \mathbf{u})^2}{2c_s^4} - \frac{(\mathbf{u} \cdot \mathbf{u})}{2c_s^2} \right], \qquad (2)$$

t_α being a weighting factor. In the above, $\mathbf{F}$ is the averaged external force experienced by each particle. In the case of a van der Waals fluid without the effect of gravity, the intermolecular attraction through the mean field approximation and the exclusion volume of molecules yield the external force [5]

$$\mathbf{F} = \nabla \left(\rho c_s^2 - p_0 \right) + \rho \kappa \nabla \nabla^2 \rho, \qquad (3)$$

where κ is the gradient parameter and p_0 is the thermodynamic pressure that separates phases. We call this form the pressure form of the intermolecular force, or simply the pressure form.

In this model, phase separation is induced by mechanical instability in the supernodal curve of the phase diagram. Unfortunately, He and coworkers [15] reported numerical instability due to the stiffness of $\mathbf{F}$. Lee and Lin [7] later showed that the compact and isotropic finite difference yields stable discretization as long as the mechanically unstable region is resolved with enough grid points. The first term of $\mathbf{F}$ is to cancel out with the ideal gas contribution to the pressure. It is not responsible for the parasitic currents but may cause serious numerical instability when an inappropriate discretization scheme is used. The second term, the thermodynamic pressure gradient, is mechanically unstable in the narrow interfacial region, in which $\partial p_0 / \partial \rho$ changes its sign. The number of grid points in this region should be chosen large enough to resolve the change. The third term is associated to the interfacial stress and should balance the thermodynamic pressure gradient to maintain the equilibrium interface profile. Without this term, the interface profile would be a step function, which is numerically unsustainable unless artificial smearing of the interface is introduced, sacrificing accuracy. We note that the interfacial stress term alone does not trigger the parasitic currents. The parasitic currents are initiated by a slight imbalance between the thermodynamic pressure gradient term and the interfacial stress term as a result of truncation error.

To avoid the truncation error, we recast Eq. (3) in the same form as the interfacial stress term using the thermodynamic identity. The mixing energy per unit volume for the isothermal system is

$$E_{mix}(\rho, \nabla\rho) = E_0(\rho) + \frac{\kappa}{2} |\nabla \rho|^2, \qquad (4)$$

where the bulk energy E_0 is related to the thermodynamic pressure p_0 by the equation of state (EOS), and the chemical potential is the derivative of the bulk energy with respect to the density:

$$p_0 = \rho \frac{\partial E_0}{\partial \rho} - E_0, \quad \mu_0 = \frac{\partial E_0}{\partial \rho}. \tag{5}$$

Using the relations Eq. (5), one can rewrite Eq. (3) in the potential form:

$$\mathbf{F} = \nabla \rho c_s^2 - \rho \nabla \left(\mu_0 - \kappa \nabla^2 \rho \right). \tag{6}$$

The equilibrium profile is determined such that the energy is minimized. Now $\mu = \mu_0 - \kappa \nabla^2 \rho$ is treated as a scalar and discretized in like manner.

In the vicinity of the critical point, EOS can be simplified [16] for control of the interface thickness and surface tension at equilibrium. We assume that the bulk energy E_0 is

$$E_0(\rho) \approx \beta \left(\rho - \rho_v^{sat} \right)^2 \left(\rho - \rho_l^{sat} \right)^2, \tag{7}$$

where β is a constant that is related to the compressibility of bulk phases, and ρ_l^{sat} and ρ_l^{sat} are the densities of vapor and liquid phases at saturation, respectively. In a plane interface at equilibrium, the density profile across the interface is

$$\rho(z) = \frac{\rho_l^{sat} + \rho_v^{sat}}{2} + \frac{\rho_l^{sat} - \rho_v^{sat}}{2} \tanh\left(\frac{2z}{D} \right), \tag{8}$$

where D is the interface thickness, which is chosen based on accuracy and stability. Given D, β, and the saturation densities, one can compute the gradient parameter κ and the surface tension force σ

$$\kappa = \frac{\beta D^2 (\rho_l^{sat} - \rho_v^{sat})^2}{8}, \quad \sigma = \frac{(\rho_l^{sat} - \rho_v^{sat})^3}{6} \sqrt{2\kappa\beta}. \tag{9}$$

In the limiting case of zero κ, the interface thickness D goes to zero. The above simplification may cease to be valid away from the critical point, namely, at large density difference or equivalently low temperature. In our experience, the numerically sustainable interface thickness is $D > 3$, below which the LBE method becomes unstable or the interface shape is distorted. At large density difference, either β or σ is compromised because of the lower bound for D. Since the speed of sound is related to the bulk energy, changing β implies modification of the speed of sound of the bulk fluid.

LBE is obtained by discretizing Eq. (1) along characteristics over the time step δt:

$$\begin{aligned} &f_\alpha(\mathbf{x} + \mathbf{e}_\alpha \delta t, t + \delta t) - f_\alpha(\mathbf{x}, t) \\ &= -\int_t^{t+\delta t} \frac{f_\alpha - f_\alpha^{eq}}{\lambda} dt' + \int_t^{t+\delta t} \frac{(\mathbf{e}_\alpha - \mathbf{u}) \cdot \left(\nabla \rho c_s^2 - \rho \nabla \mu \right)}{\rho c_s^2} f_\alpha^{eq} dt'. \end{aligned} \tag{10}$$

The time integration in $[t, t+\delta t]$ is coupled with the space integration in $[\mathbf{x}, \mathbf{x} + \mathbf{e}_\alpha \delta t]$. Application of the trapezoidal rule for second-order accuracy and unconditional stability leads to

$$\begin{aligned} &f_\alpha(\mathbf{x} + \mathbf{e}_\alpha \delta t, t + \delta t) - f_\alpha(\mathbf{x}, t) \\ &= -\frac{f_\alpha - f_\alpha^{eq}}{2\tau}\Big|_{(\mathbf{x},t)} - \frac{f_\alpha - f_\alpha^{eq}}{2\tau}\Big|_{(\mathbf{x}+\mathbf{e}_\alpha \delta t, t+\delta t)} \\ &\quad + \frac{\delta t}{2} \frac{(\mathbf{e}_\alpha - \mathbf{u}) \cdot \left(\nabla \rho c_s^2 - \rho \nabla \mu \right)}{\rho c_s^2} f_\alpha^{eq}\Big|_{(\mathbf{x},t)} \\ &\quad + \frac{\delta t}{2} \frac{(\mathbf{e}_\alpha - \mathbf{u}) \cdot \left(\nabla \rho c_s^2 - \rho \nabla \mu \right)}{\rho c_s^2} f_\alpha^{eq}\Big|_{(\mathbf{x}+\mathbf{e}_\alpha \delta t, t+\delta t)}, \end{aligned} \tag{11}$$

where the nondimensional relaxation time $\tau = \lambda / \delta t$ and is related to the kinematic viscosity by $\nu = \tau c_s^2 \delta t$.

The space discretization of $\delta t \mathbf{e}_\alpha \cdot \nabla \rho$ and $\delta t \mathbf{e}_\alpha \cdot \rho \nabla \mu$ is of critical importance to stability and elimination of the parasitic currents. Lee and Lin [7] showed that discretizations of these directional derivatives at $(\mathbf{x} + \mathbf{e}_\alpha \delta t)$ and $(\mathbf{x})$ should be compact around $(\mathbf{x} + \mathbf{e}_\alpha \delta t)$:

$$\begin{aligned} \delta t \mathbf{e}_\alpha \cdot \nabla \rho|_{(\mathbf{x}+\mathbf{e}_\alpha \delta t)} &= \frac{\rho(\mathbf{x}+\mathbf{e}_\alpha \delta t) - \rho(\mathbf{x}+\mathbf{e}_\alpha \delta t)}{2}, \\ \delta t \mathbf{e}_\alpha \cdot \nabla \rho|_{(\mathbf{x})} &= \frac{-\rho(\mathbf{x}+2\mathbf{e}_\alpha \delta t) + 4\rho(\mathbf{x}+\mathbf{e}_\alpha \delta t) - 3\rho(\mathbf{x})}{2}. \end{aligned} \tag{12}$$

Finite differences in Eq.(13) are second-order accurate and require only three lattice sites around $(\mathbf{x} + \mathbf{e}_\alpha \delta t)$. In Eq. (13), a backward characteristic approximation is used. Derivatives other than the directional derivatives can be obtained by taking moments of the 1-D second-order central difference along characteristics. Specifically, the first and the second derivatives are discretized as follows:

$$\begin{aligned} \nabla \rho|_{(\mathbf{x})} &= \textstyle\sum_{\alpha \neq 0} \frac{t_\alpha \mathbf{e}_\alpha [\rho(\mathbf{x}+\mathbf{e}_\alpha \delta t) - \rho(\mathbf{x}-\mathbf{e}_\alpha \delta t)]}{2 c_s^2 \delta t}, \\ \nabla^2 \rho|_{(\mathbf{x})} &= \textstyle\sum_{\alpha \neq 0} \frac{t_\alpha [\rho(\mathbf{x}+\mathbf{e}_\alpha \delta t) - 2\rho(\mathbf{x}) + \rho(\mathbf{x}-\mathbf{e}_\alpha \delta t)]}{c_s^2 \delta t^2}. \end{aligned} \tag{13}$$

The isotropic discretization in LBE and its force terms prevents the parasitic currents from developing into organized eddies.

Here, we introduce modified particle distribution function $\bar{f}_\alpha$ and equilibrium distribution function $\bar{f}_\alpha^{eq}$ to facilitate computation:

$$\begin{aligned} \bar{f}_\alpha &= f_\alpha + \frac{f_\alpha - f_\alpha^{eq}}{2\tau} - \frac{\delta t}{2} \frac{(\mathbf{e}_\alpha - \mathbf{u}) \cdot \left(\nabla \rho c_s^2 - \rho \nabla \mu \right)}{\rho c_s^2} f_\alpha^{eq}, \\ \bar{f}_\alpha^{eq} &= f_\alpha^{eq} - \frac{\delta t}{2} \frac{(\mathbf{e}_\alpha - \mathbf{u}) \cdot \left(\nabla \rho c_s^2 - \rho \nabla \mu \right)}{\rho c_s^2} f_\alpha^{eq}. \end{aligned} \tag{14}$$

Note that $\delta t \mathbf{e}_\alpha \cdot \nabla\rho$ and $\delta t \mathbf{e}_\alpha \cdot \rho\nabla\mu$ in the definition of the modified equilibrium distribution $\bar{f}_\alpha^{eq}$ should be discretized by the central difference. The density and the momentum can be computed by taking the zeroth and first moments of the modified particle distribution function:

$$\begin{aligned} \rho &= \textstyle\sum_\alpha f_\alpha = \sum_\alpha \bar{f}_\alpha, \\ \rho\mathbf{u} &= \textstyle\sum_\alpha \mathbf{e}_\alpha f_\alpha = \sum_\alpha \mathbf{e}_\alpha \bar{f}_\alpha + \frac{\delta t}{2}\left(\nabla\rho c_s^2 - \rho\nabla\mu\right). \end{aligned} \tag{15}$$

The above LBE can then be recast in a simpler form:

$$\begin{aligned} \bar{f}_\alpha(\mathbf{x}+\mathbf{e}_\alpha\delta t, t+\delta t) - \bar{f}_\alpha(\mathbf{x},t) &= -\tfrac{1}{\tau+0.5}\left(\bar{f}_\alpha - \bar{f}_\alpha^{eq}\right)|_{(\mathbf{x},t)} \\ &+ \tfrac{(\mathbf{e}_\alpha-\mathbf{u})\cdot\left(\nabla\rho c_s^2 - \rho\nabla\mu\right)}{\rho c_s^2} f_\alpha^{eq}|_{(\mathbf{x},t)}\delta t. \end{aligned} \tag{16}$$

Although the above equation appears to be explicit in time, it is fully implicit for the relaxation term and the intermolecular force terms alike and, therefore, is unconditionally stable and second order accurate. The directional derivatives in the force terms are discretized by the mixed difference, for instance,

$$\begin{aligned} \mathbf{e}_\alpha \cdot \nabla\rho|_{(\mathbf{x})} &= \tfrac{[\rho(\mathbf{x}+\mathbf{e}_\alpha\delta t) - \rho(\mathbf{x}-\mathbf{e}_\alpha\delta t)]}{4\delta t} \\ &+ \tfrac{[-\rho(\mathbf{x}+2\mathbf{e}_\alpha\delta t) + 4\rho(\mathbf{x}+\mathbf{e}_\alpha\delta t) - 3\rho(\mathbf{x})]}{4\delta t}. \end{aligned} \tag{17}$$

NUMERICAL TEST

The test cases confirm that the LBE with the potential form is able to reach an equilibrium. Figure 1 shows $\rho\mathbf{u}$ fields after $100,000$ time steps are plotted, when steady-state solutions are assumed. As initial conditions, a 2-D droplet is generated on 100×100 periodic computational domain for a D2Q9 lattice. The interface thickness, droplet radius, and relaxation time are $D = 4$, $R_0 = 25$, and $\tau = 0.5$, respectively. We fixed $\beta = 0.01$, $\rho_l^{sat} = 1.0$, and $\rho_v^{sat} = 0.1$, in which case the surface tension is $\sigma = 2.187 \times 10^{-3}$. Values of $\rho\mathbf{u}$ are magnified by 2×10^5 times in (a) and 1×10^{15} times in (b). Figure 1(a) indicates the presence of parasitic currents that are roughly aligned in the direction normal to the interface, when the pressure form of the intermolecular force is used. Away from the interface, the parasitic currents rapidly disappear. Inexact satisfaction of $\nabla p_0 = \rho\nabla\mu_0$ is responsible for the parasitic currents. Following the analysis of Jamet *et al*. [11], the discretized relation for $\nabla p_0|_{(\mathbf{x})} = \rho\nabla\mu_0|_{(\mathbf{x})}$ should be

$$\begin{aligned} &\textstyle\sum_{\alpha\neq 0} \frac{t_\alpha \mathbf{e}_\alpha [p_0(\mathbf{x}+\mathbf{e}_\alpha\delta t) - p_0(\mathbf{x}-\mathbf{e}_\alpha\delta t)]}{2c_s^2\delta t} \\ &= \textstyle\sum_{\alpha\neq 0} \frac{t_\alpha \mathbf{e}_\alpha \rho [\mu_0(\mathbf{x}+\mathbf{e}_\alpha\delta t) - \mu_0(\mathbf{x}-\mathbf{e}_\alpha\delta t)]}{2c_s^2\delta t}. \end{aligned} \tag{18}$$

(a) Pressure form

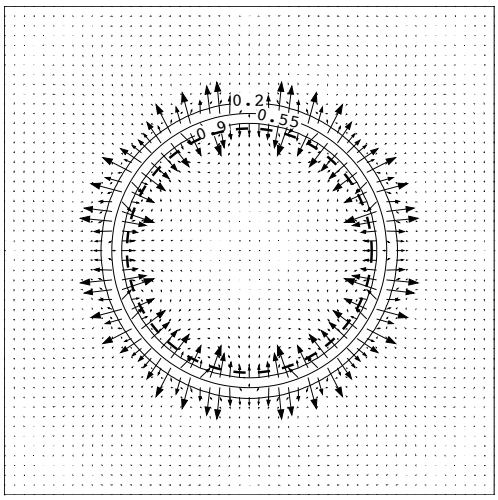

(b) Potential form

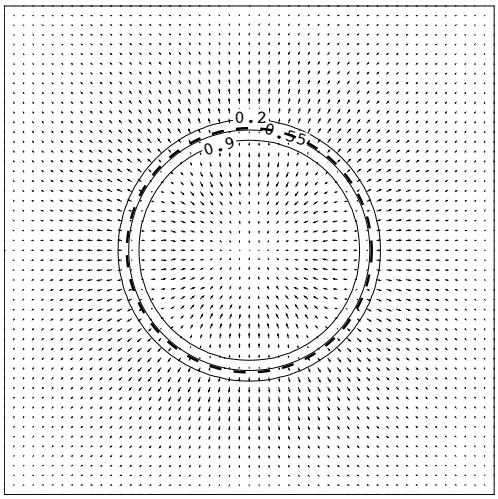

Figure 1. $\rho\mathbf{u}$ FIELDS AFTER $100,000$ TIME STEPS ON 100×100 LATTICE AT $D = 4$, $R_0 = 25$, $\tau = 0.5$, $\beta = 0.01$, $\rho_l^{sat} = 1.0$, and $\rho_v^{sat} = 0.1$. VALUES OF $\rho\mathbf{u}$ ARE MAGNIFIED BY 2×10^5 TIMES IN (a) AND 1×10^{15} TIMES (b).

However, the Taylor-series expanding the pressure and the chemical potential reveals that the truncation error is proportional to the density gradients:

$$\nabla p_0|_{(\mathbf{x})} - \rho\nabla\mu_0|_{(\mathbf{x})} = \sum_{\alpha\neq 0} \frac{t_\alpha \mathbf{e}_\alpha}{6c_s^2\delta t}\left[\left(\frac{\partial\mu_0}{\partial\rho}\right)(\delta t\mathbf{e}_\alpha\cdot\nabla\rho)(\delta t\mathbf{e}_\alpha\cdot\nabla)^2\rho\right]_{(\mathbf{x})}. \tag{19}$$

We observe that the flow does not exhibit any organized eddies despite the presence of parasitic currents. We speculate that the absence of eddies is due to the isotropic discretization of LBE.

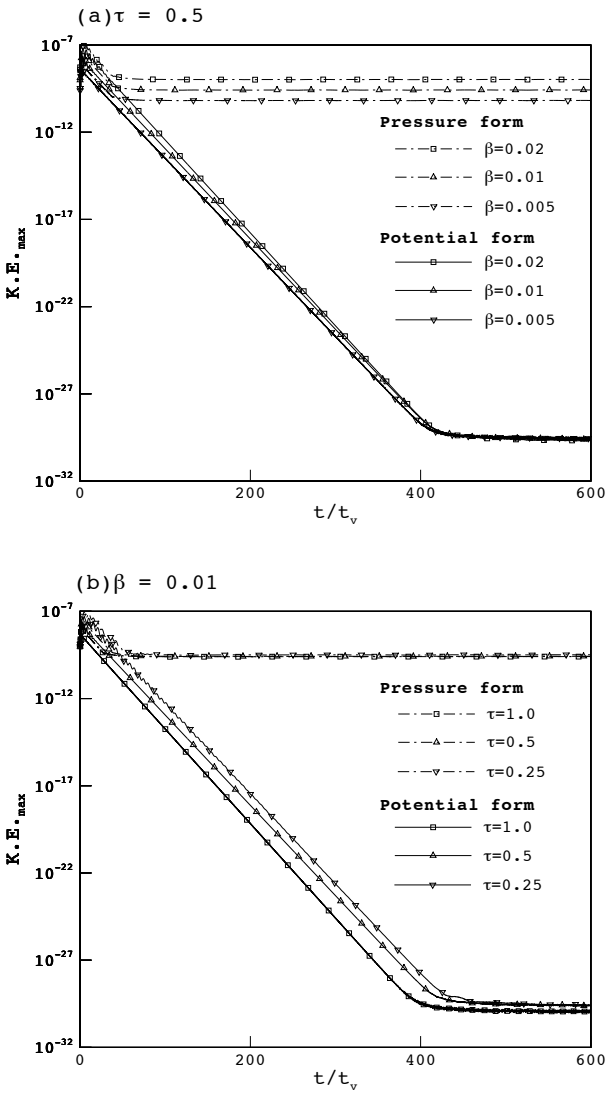

Figure 2. TIME EVOLUTION OF THE MAXIMUM KINETIC ENERGY FOR A POTENTIAL FORM AND A PRESSURE FORM OF THE INTERMOLECULAR FORCE AT $D = 4$, $R_0 = 25$, $\rho_l^{sat} = 1.0$, AND $\rho_v^{sat} = 0.1$. TIME IS NONDIMENSIONALIZED TO THE VISCOUS TIME OF THE VAPOR PHASE $t_v = \rho_v^{sat} \nu_v^{sat} R_0/\sigma$. τ IS FIXED AT 0.5 IN (a), AND THE SURFACE TENSION FORCES ARE $\sigma = 4.374 \times 10^{-3}, 2.187 \times 10^{-3}$, AND 1.094×10^{-3} IN THE DESCENDING ORDER OF β. IN (b) β IS FIXED AT 0.01.

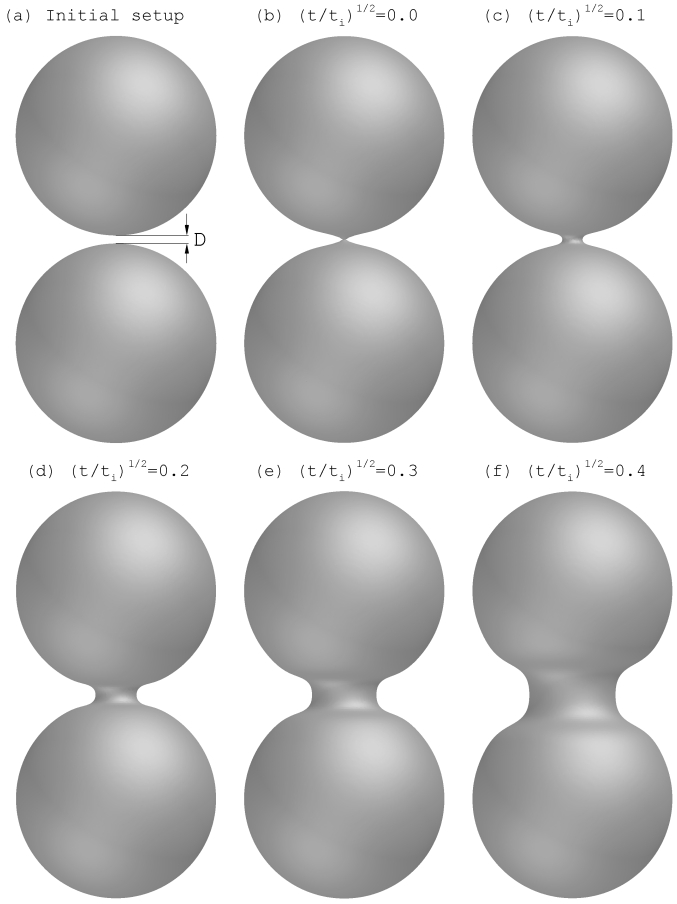

Figure 3. COALESCENCE OF TWO DROPLETS ON $200 \times 400 \times 200$ LATTICE $D = 4$, $R_0 = 50$, $\beta = 0.02$, $\tau_l^{sat} = 0.01$, $\tau_v^{sat} = 0.2$, $\rho_l^{sat} = 1.0$, AND $\rho_v^{sat} = 0.001$. TIME IS NONDIMENSIONALIZED TO THE INERTIAL TIME OF THE LIQUID PHASE $t_i = \sqrt{\rho_l^{sat} R_0^3/\sigma}$.

The magnitude of the currents may be small, but the most undesirable outcome of the parasitic currents is the violation of mass conservation. Fig. 1(a) shows that the droplet radius is increased after long time integration. Ideally, the net balance of mass flux across the interface region should be zero, even if values of $\rho\mathbf{u}$ remain finite. The potential form eliminates the parasitic currents, as numerically confirmed in Fig. 1(b). The radius of the droplet is also well maintained. Effects of β on the parasitic currents are examined in Fig. 2(a). The relaxation time and the interface thickness are fixed at $\tau = 0.5$ and $D = 4$, respectively. By fixing τ, the viscosity of the fluid is fixed. Given the interface thickness and the density ratio, higher β means higher surface tension force as well as less compressibility, thus implying faster convergence rate. When the time is nondimensionalized to the viscous time of the vapor phase $t_v = \rho_v^{sat} \nu_v^{sat} R_0/\sigma$, the convergence rates for different β and models collapse on a single curve. The maximum kinetic energy with the potential form decreases exponentially to round-off. On the contrary, the maximum kinetic energy with the pressure form initially decreases at the same rate as that of the potential form, but eventually stagnates. The maximum steady-state kinetic energy of the pressure form decreases with β, as the surface tension force decreases accordingly. A similar trend can be found when β is fixed and the relaxation time τ is varied in Fig. 2(b).

To test stability of the proposed model, we examine inertial

coalescence of droplets, driven by the surface tension. Industrial applications of this process may include emulsion stability, inkjet printing, and coating applications. At the moment of contact of droplets, the inversion of radius of curvature causes a singularity, forming a liquid bridge between the droplets. The radius of the liquid bridge R_0 then grows as $R_0(t) \propto \sqrt{t}$ by equating capillary and inertial forces. Aarts *et al.* [17] experimentally found the following prefactors for the scaling relation: water, 1.14; 5 mPa s silicon oil, 1.24; and 20 mPa s silicon oil, 1.11. Inviscid incompressible simulation by Duchemin*et al.* [18] predicted a rather large prefactor of 1.62. The initialization of simulation of coalescence is particularly challenging. Duchemin *et al.* [18] and Menchaca-Rocha *et al.* [19] smoothed the interface profile in the region of liquid bridge to avoid infinitely large capillary forces caused by the singular curvature. An effect of smoothing could be slower initial growth of the radius of the liquid bridge as a result of smaller capillary forces.

Instead of smoothing the initial profile, we choose to separate two stationary droplets by the equilibrium interface thickness D as shown in Figure 3(a). The intermolecular attraction acts at this distance and initiates the formation of the liquid bridge. Fig. 3 shows coalescence of two droplets. Two 3-D droplets are generated on a $200 \times 400 \times 200$ periodic computational domain for a D3Q27 lattice. The interface thickness, droplet radius, and relaxation times for liquid and vapor phases are $D = 4$, $R_0 = 50$, and $\tau_l^{sat} = 0.01$ and $\tau_v^{sat} = 0.2$, respectively. We fixed $\beta = 0.02$, $\rho_l^{sat} = 1.0$, and $\rho_v^{sat} = 0.001$. Time is nondimensionalized to the inertial time of the liquid phase $t_i = \sqrt{\rho_l^{sat} R_0^3/\sigma}$ [18] and is measured from the moment of contact (Fig. 3(b)). The results are in good qualitative agreement with previous experimental results [17, 18], except for the elongated neck region due to initial separation. The finite value of the initial separation relative to the radius of droplets can be reduced by adopting a finer mesh or an adaptive mesh refinement.

Although the approach based on free energy is derived to describe the near-critical behavior of nonideal gases at small density ratio, it is generally believed to be valid even when the density gradients become large [20]. As β decreases in the present model, however, the approximation of the bulk energy by Eq. (7) may become inaccurate. The effect of β on the inertial coalescence of droplets plotted in Fig. 4, shows time evolution of the nondimensionalized neck radii for $\beta = 0.02$, 0.01, and 0.005. The differences in the results are negligible in this range of β. The radii of the neck converge to the line whose slope is 1.2 [17] after rapid early growth, which is governed by the singular curvature at the moment of contact. Using an inviscid incompressible numerical method, Menchaca-Rocha *et al.* [19] reported slower initial growth of the neck radius, followed by transition region.

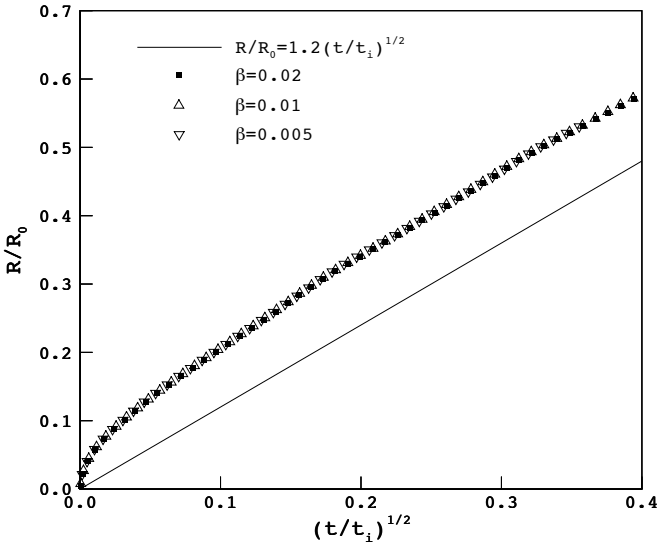

Figure 4. TIME EVOLUTION OF THE RADIUS OF THE NECK FOR INERTIA DOMINATED FLOWS. THE FULL LINE HAS A SLOPE OF 1.2 [17].

CONCLUDING REMARKS

Two sources of error in the computation of the surface tension force lead to development of the parasitic currents. A slight imbalance between the pressure gradient and the stresses due to truncation error initiates the parasitic currents. As long as isotropy of the numerical scheme is retained, the parasitic currents are kept aligned in the direction normal to the interface. If isotropy is not maintained, however, the parasitic currents eventually develop into the organized flow patterns. The LBE method with isotropic discretizations can avoid formation of organized flow patterns. Furthermore, the use of the potential form of the intermolecular force eliminates the parasitic currents to roundoff.

The present LBE model is applied to the simulation of droplet coalescence in order to demonstrate its stability at high density ratio. The results show that the evolution of the computed neck radius follows the experimental growth rate, but deviates from the growth rate determined by inviscid incompressible numerical calculation. This deviation can be attributed to the incompressibility in the interface region and the initial profile of droplets.

ACKNOWLEDGMENT

This work was supported in part by the Mathematical, Information, and Computational Sciences Division subprogram of the Office of Advanced Computing Research, Office of Science, U.S. Dept. of Energy, under Contract W-31-109-Eng-38.

REFERENCES

[1] Gunstensen, A., Rothman, D., Zaleski, S., and Zanetti, G., 1991. "A discrete Boltzmann equation model for non-ideal gases". *Phys. Rev. A,* **43**, p. 4320.

[2] Shan, X., and Chen, H., 1993. "Lattice Boltzmann model for simulating flows with multiple phases and components". *Phys. Rev. E,* **47**, p. 1815.

[3] Swift, M., Osborn, W., and Yeomans, J., 1995. "Lattice Boltzmann simulation of nonideal fluids". *Phys. Rev. Lett.,* **75**, p. 830.

[4] Martys, N., and Chen, H., 1996. "Simulation of multicomponent fluids in complex three-dimensional geometries by the lattice Boltzmann method". *Phys. Rev. E,* **53**, p. 743.

[5] He, X., Chen, S., and Doolen, G., 1998. "A discrete Boltzmann equation model for non-ideal gases". *Phys. Rev. E,* **57**, p. R13.

[6] Luo, L.-S., 1998. "Unified theory of lattice Boltzmann models for nonideal gases". *Phys. Rev. Lett.,* **81**, p. 1618.

[7] Lee, T., and Lin, C.-L., 2005. "A stable discretization of the lattice Boltzmann equation for simulation of incompressible two-phase flows at high density ratio". *J. Comput. Phys.,* **206**, p. 16.

[8] Anderson, D., McFadden, G., and Wheeler, A., 1998. "Diffuse-interface methods in fluid mechanics". *Annu. Rev. Fluid Mech.,* **30**, p. 139.

[9] Lafaurie, B., Nardone, C., Scardovelli, R., Zaleski, S., and Zanetti, G., 1994. "Modeling merging and fragmentation in multiphase flows with SURFER". *J. Comput. Phys.,* **113**, p. 134.

[10] Jacqmin, D., 1996. "An energy approach to the continuum surface tension method". *AIAA paper 96-0858*.

[11] Jamet, D., Torres, D., and Brackbill, J., 2002. "On the theory and computation of surface tension: The elimination of parasitic currents through energy conservation in the second-gradient method". *J. Comput. Phys.,* **182**, p. 276.

[12] Nourgaliev, R., Dinh, T., and Sehgal, B., 2002. "On lattice boltzmann modeling of phase transition in an isothermal non-ideal fluid". *Nuclear Engrg. and Design,* **211**, p. 153.

[13] Lishchuk, S., Care, C., and Halliday, I., 2003. "Lattice Boltzmann algorithm for surface tension with greatly reduced microcurrents". *Phys. Rev. E,* **67**, p. 036701.

[14] Cristea, A., and Sofonea, V., 2003. "Reduction of spurious velocity in finite difference lattice boltzmann models for liquid-vapor systems". *Int. J. Mod. Phys. C,* **14**, p. 1251.

[15] X. He, S. C., and Zhang, R., 1999. "A lattice Boltzmann scheme for incompressible multiphase flow and its application in simulation of Rayleigh-Taylor instability". *J. Comput. Phys.,* **152**, p. 642.

[16] Rowlinson, J., and Widom, B., 2002. "Moleculary theory of capillarity". *Dover Publications, Inc., New York*.

[17] Aarts, D., Lekkerkerker, H., Guo, H., Wegdam, G., and Bonn, D., 2005. "Hydrodynamics of droplet coalescence". *Phys. Rev. Lett.,* **95**, p. 16503.

[18] Duchemin, L., Eggers, J., and Josserand, C., 2003. "Inviscid coalescence of drops". *J. Fluid Mech.,* **487**, p. 167.

[19] Menchaca-Rocha, A., Martínez-Dávalos, A., Núñez, R., Popinet, S., and Zaleski, S., 2003. "Coalescence of liquid drops by surface tension". *Phys. Rev. E,* **63**, p. 046309.

[20] Lowengrub, J., and Truskinovsky, L., 1998. "Quasi-incompressible Cahn-Hilliard fluids and topological transitions". *Proc. R. Soc. Lond. A,* **454**, p. 2617.